JOURNAL OF MATERIALS SCIENCE **38** (2003) 2633–2638

Metalorganic chemical vapor deposition of $SrRuO_3$ thin film and its characterization

HUNG-CHIH LEE, DAH-SHYANG TSAI*
Department of Chemical Engineering, National Taiwan, University of Science and Technology, 43 Keelung Road, Section 4, Taipei, Taiwan, Republic of China
E-mail: tsai@ch.ntust.edu.tw

Synthesis of conducting oxide strontium ruthenate is carried out in a hot-wall tubular reactor, using $Sr(C_{11}H_{19}O_2)_2/Ru(C_5H_5)_2/O_2$ reaction system. Owing to a large difference in depositing efficiency between strontium and ruthenium precursors, the stoichiometric ratio of thin film is controlled in one cycle of two consecutive depositions at different temperatures. Thin films of $SrRuO_3$ single phase are synthesized in the subsequent 700°C annealing. Thin films of $SrRuO_3$ with extra ruthenium oxide can also be prepared by adjusting the molar ratio of RuO_2 and SrO layers. The deposition sequence of ruthenium oxide first, strontium oxide later is preferred. If the deposition sequence is reverse, the thin film is plagued with unreacted oxides even when the annealing temperature is raised to 800°C. The relative ease of preparing $SrRuO_3$ thin films, when RuO_2 is under SrO, is attributed to evaporation of ruthenium oxide in O_2 and diffusion in its open columnar microstructure. The sheet resistivity of thin film decreases with the ruthenium content. The room temperature resistivity of $SrRuO_3$ film of $Ru/(Sr + Ru) = 0.5$ is around 910 μohm-cm. The room-temperature resistivity of $Ru/(Ru + Sr) = 0.53$ decreases to 470 μohm-cm. The root mean square surface roughness of 700°C synthesized $SrRuO_3$ thin film is 22 nm, in a 2×2 μm^2 area of film thickness 280 nm.

1. Introduction

The perovskite strontium ruthenate, which crystallizes in $GdFeO_3$-type orthorhombic structure with space group *Pbnm*, is of interests owing to its metallic conductivity and ferromagnetism at low temperatures [1–3]. A combination of good chemical stability, low electrical resistivity, and epitaxial growth on other ferroelectric perovskites make it an attractive candidate for bottom electrode of the ferroelectric capacitor, also buffer layer for growing $YBa_2Cu_3O_7$ superconductor. The microstructure and properties of sputtered $SrRuO_3$ thin film have been studied, and its feasibility as electrode for (Ba,Sr)TiO_3 and Pb(Zr,Ti)O_3 dielectrics has been evaluated [4–6]. Considerable alleviation of polarization fatigue problem on ferroelectric capacitor with $SrRuO_3$ electrode has been reported [6–9]. Well-textured and epitaxial films have been synthesized, using pulsed laser deposition PLD and RF sputtering [10, 11].

The synthesis of $SrRuO_3$ thin film via chemical routes, on the other hand, seems to be troublesome. Polycrystalline films of mixed phases $SrRuO_3$, Sr_2RuO_4, and RuO_2 have been deposited on silicon and aluminum oxide substrates, using a tubular hot-wall reactor. The electrical resistivity of film is significantly higher than those prepared by PLD owing to the difficulty in stoichiometric control [12]. Unidentified extra phases in $SrRuO_3$ powders and thin films have been reported in the sol-gel processing of strontium and ruthenium acetylacetonate [13]. A better composition control has been achieved in an metalorganic CVD cold-wall reactor, using pecursors $Sr(C_{11}H_{19}O_2)_2(C_8H_{23}N_5)_2$ and $Ru(C_{11}H_{19}O_2)_3$. The resistivity of synthesized film, which has been deposited on $LaAlO_3$ substrate at 750°C, is strongly influenced by the $Ru/(Ru + Sr)$ ratio [14].

In this paper, we study the preparation of $SrRuO_3$ thin films using metalorganic CVD. The molar ratio of thin film is controlled by depositing its component oxides separately, then two oxides react in the high-temperature annealing. The reactivity difference between Ru and Sr precursors becomes less problematic in this approach. The microstructure and electrical properties of the prepared thin films are measured and discussed.

2. Experimental

2.1. Thin film preparation

Thin films of $SrRuO_3$, RuO_2 and SrO were grown on (100) silicon wafer placed in a long quartz tube of diameter 29 mm, which was heated in a three-zone hot-wall furnace. The wafer substrate, of width 8 mm and length 20–25 mm, was thermally oxidized and cleaned before

*Author to whom all correspondence should be addressed.

being placed in the reactor. The temperature of hot zone was controlled within ±2°C. The organometallic precursors were bis(di-pivaloylmethanato) strontium $Sr(thd)_2$ (purity > 99.99%, Chemat Technology, Northridge, California) and ruthenocene $Ru(C_5H_5)_2$ (purity > 99%, Strem Chemicals, Newburyport, Massachusetts), both are in form of powder. The two solid precursors were sublimed separately at upstream positions in front of the hot zone. The sublimation temperature was 220°C for $Sr(thd)_2$, 80°C for ruthenocene. The precursor vapor was carried into the reactor by flowing oxygen with a fixed flow rate 190 sccm. The total pressure was fixed at 4.8 Torr. Two oxides could be deposited simultaneously or separately. If they were deposited separately, annealing in flowing oxygen is necessary to prepare strontium ruthenate. The annealing temperature was set between 550 and 800°C, with oxygen flow rate 180 sccm and total pressure 4.5 Torr. When RuO_2 was deposited alone the hot-zone temperature was between 200 and 355°C, while SrO was deposited at a higher temperature, 450 and 550°C. It was important to maintain the flowing oxygen throughout the deposition cycle, since RuO_2 could easily be reduced to metal without oxygen under elevated temperatures. The oxygen source was turned off at the end of cycle when the furnace was cooled down to 100°C.

2.2. Microstructural observation and property measurement

The surface morphology and the cross section of deposited film were examined under a scanning electron microscope SEM (XL30, Philips). The surface topography was observed over an area of $2 \times 2\ \mu m^2$, using an atomic force microscope (Nanoscope III, Digital Instrument). The crystal phase of thin film was inspected by X-ray diffractometry (D/Max, Rigaku, Cu K_α radiation source). Its composition was measured by X-ray photoelectron spectroscopy (XPS, VG MT-500). The molar ratio was determined by deconvoluting the peak areas of Sr $3d_{5/2}$ and $3d_{3/2}$ and Ru $3d_{5/2}$ and $3d_{3/2}$, using XPS software Matalab (version 3.5). The sheet resistance of thin film was measured by the van der Pauw method, using a four-point probe and a helium cooling system (temperature range 17–300 K).

3. Results and discussion

3.1. Synthesis of strontium ruthenate

When RuO_2 and SrO are deposited individually in a tubular reactor with flowing oxygen, ruthenium oxide is deposited at much lower temperatures than strontium oxide owing to its higher deposition efficiency. Ruthenium oxide can be grown via $Ru(C_5H_5)_2$ at a temperature as low as 200°C, as reported by Shin and Yoon [15]. On the other hand, appreciable strontium oxide does not grown until the hot-zone temperature is over 400°C, using $Sr(thd)_2$. Hence, when the $Ru(C_5H_5)_2$ and the $Sr(thd)_2$ precursors sublime simultaneously and deposit under the same hot-zone temperature, Sr/Ru ratio of the thin film varies considerably in the axial direction. RuO_2 tends to deposit at upstream positions, while SrO deposits at downstream positions. A section of thin film grown at 430°C, in between the RuO_2-rich region and the SrO-rich region, exhibits an evident two-layer morphology, shown in Fig. 1. This cross-section of thin film is featured with a dense microstructure on top of a columnar structure. Elemental analysis indicates that the top dense microstructure is almost all strontium, and the underneath columnar structure is ruthenium-rich. Apparently, the higher volatility of ruthenocene and the higher deposition efficiency cause ruthenocene depletes first and most of RuO_2 deposits before SrO does. The X-ray diffraction pattern of this thin film in Fig. 1 is illustrated in Fig. 2a. Six rather broad $SrCO_3$ reflections (JCPDS 05-0418) and four narrow RuO_2 reflections (JCPDS 43-1027) are identified in Fig. 2a. The presence of strontium carbonate results from the reaction between SrO and CO_2 in the ambient air. The absorption of carbon dioxide causes the shiny surface of as-prepared thin film becomes hazy, which occurs several days after the wafer was taken out the CVD reactor.

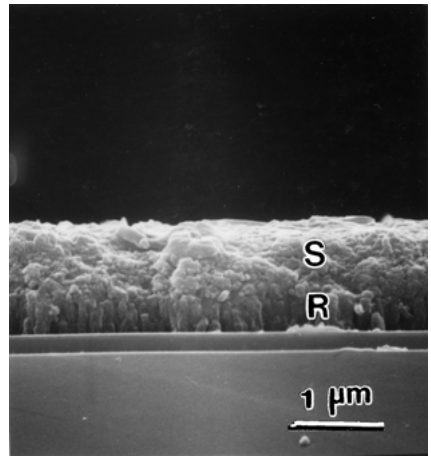

Figure 1 Micrographs of the thin film deposited at 430°C as $Ru(C_5H_5)_2$ and $Sr(thd)_2$ are sublimed and deposited simultaneously. The underlying RuO_2-rich region (denoted by "R") in the cross section is featured with columnar grains. The SrO-rich region is denoted by "S".

To control the composition, two oxide films are deposited to their prescribed thickness at different temperatures. The prescribed thickness of RuO_2 is 0.21 μm and that of SrO is 0.18 μm. Two oxides then undergo solid-state reaction at a higher temperature to synthesize strontium ruthenate. It turns out that the deposition sequence is important for the subsequent homogenization step. Fig. 2b shows the X-ray diffraction pattern of the thin film S550R295 after 700°C annealing, which is prepared by first depositing SrO at 550°C, then RuO_2 at 295°C. If S550R295 does not undergo annealing at a higher temperature, it contains only SrO and RuO_2, and its X-ray pattern is almost identical with Fig. 2a. Certain amount of $SrRuO_3$ forms when S550R295 is annealed at 700°C for 2 hrs. The $SrRuO_3$ content will increase if the annealing temperature is 800°C, Fig. 2c, but unreacted RuO_2 and SrO still remain in the thin film. If the deposition sequence is reversed, RuO_2 is deposited at 295°C first, then SrO at 550°C, the thin film is labeled as R295S550. The

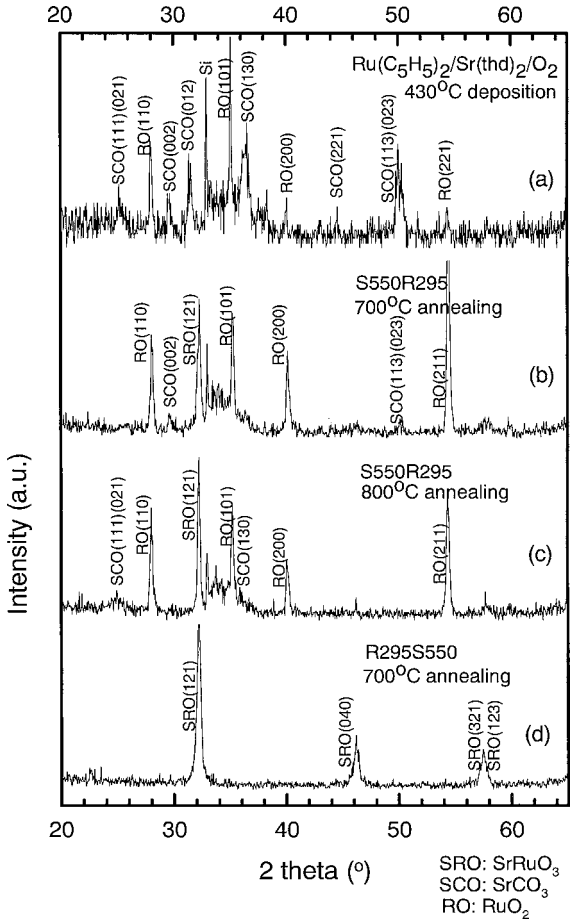

Figure 2 X-ray diffraction patterns of (a) the thin film deposited at 430°C when $Ru(C_5H_5)_2$ and $Sr(thd)_2$ are sublimed and deposited simultaneously, (b) the S550R295 thin film annealed at 700°C for 2 hrs, (c) the S550R295 thin film annealed at 800°C for 2 hrs, and (d) the R295S550 thin film annealed at 700°C for 2 hrs.

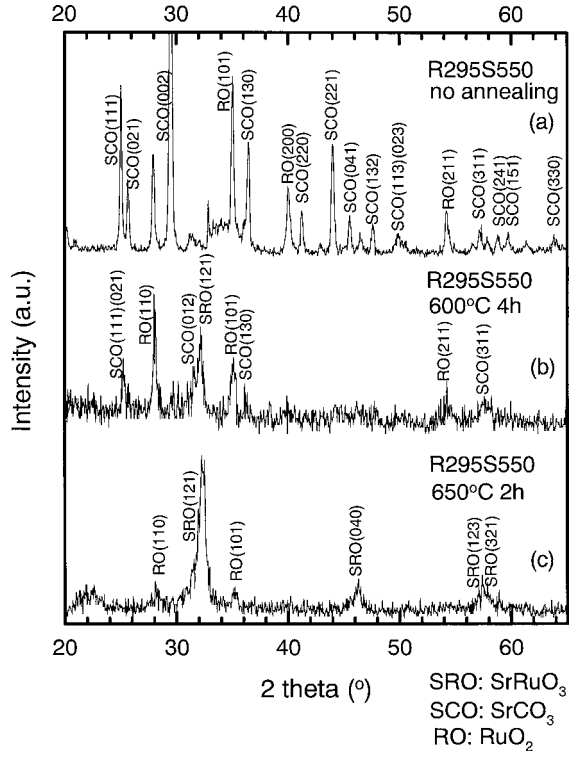

Figure 3 X-ray diffraction patterns of (a) the R295S550 thin film without annealing, (b) the R295S550 thin film annealed at 600°C for 4 hrs, and (c) the R295S550 thin film annealed at 650°C for 2 hrs.

homogenization reaction seems to be easier to proceed in the R295S550 thin film. After annealing at 700°C for 2 hrs, R295S550 can be converted to $SrRuO_3$ (JCPDS 43-0472) completely. There are no unreacted RuO_2 and $SrCO_3$ reflections detected in its X-ray diffraction pattern, illustrated in Fig. 2d. The shiny surface of $SrRuO_3$ thin film will not turn hazy after storing for several months.

Fig. 3 provides more details on R295S550 during annealing. The X-ray diffraction pattern without annealing contains both reflections of RuO_2 and $SrCO_3$, but no $SrRuO_3$ reflections, Fig. 3a. It indicates that little reaction occurs between two oxides at 550°C. The $SrRuO_3$ phase emerges at the expense of RuO_2 and SrO in the thin film of R295S550 after annealing at 600°C for 4 hrs, Fig. 3b. The reflections of RuO_2 and SrO further diminish after 650°C annealing for 2 hrs, Fig. 3c. The reflections of $SrRuO_3$ in Fig. 3b and c are rather broad. The thin films, annealed at 600 and 650°C, may contain a small amount of Sr_2RuO_4 (JCPDS 43-0217), since its major reflections are near those of $SrRuO_3$. Further raising the annealing temperature to 700°C can synthesize $SrRuO_3$ single phase of R295S550 sample, Fig. 2d.

The rate difference in synthesizing $SrRuO_3$ phase between R295S550 and S550R295 is peculiar. No rate difference is expected in exchanging the sequence of two layers, if the homogenization proceeds via solid-state diffusion and reaction alone. The plausible explanation lies in the volatility of ruthenium oxide. It has been reported that the surface morphology of RuO_2 changes when the RuO_2 thin film is annealed in oxygen at 700 and 800°C, most drastically at 800°C [16]. The microstructural change in RuO_2 is believed due to volatilization as RuO_4 and RuO_3 under high temperatures and oxygen ambient pressure [17]. The microstructure of RuO_2 thin film deposited at 315°C is illustrated in Fig. 4a. The distinct columnar structure has also been observed and reported by Shin and Yoon at 300°C [15], Liao *et al.*, at 500–550°C [18], and Chen *et al.* [19]. The RuO_2 grain size in Fig. 4a is around 110 nm. On the other hand, the microstructure of SrO film, shown in Fig. 4b, appears to be much denser and more compact than the RuO_2 columnar structure. No distinctive grain boundary in SrO thin film is observed. The SrO micrograph in Fig. 4b was taken, as soon as the thin film was retrieved from the CVD reactor, so that the $SrCO_3$ content was minimum. When R295S550 was annealed under O_2 partial pressure 4.5 Torr, the underlying RuO_2 evaporated in form of RuO_4 or RuO_3, rose up, being captured by dense SrO crystals, and formed $SrRuO_3$. For the thin film S550R295, RuO_2 is on top of SrO layer, which is a refractory oxide of melting point 2430°C. In this configuration, although RuO_2 is more probable in contact with oxygen and form RuO_4 and RuO_3 vapor, yet the vapor has less opportunity to reach SrO crystals and react. Consequently, the formation of $SrRuO_3$ in S550R295 is more difficult.

To further examine the idea of RuO_2 volatility, we prepared a sandwich film of R295S550R295 with two

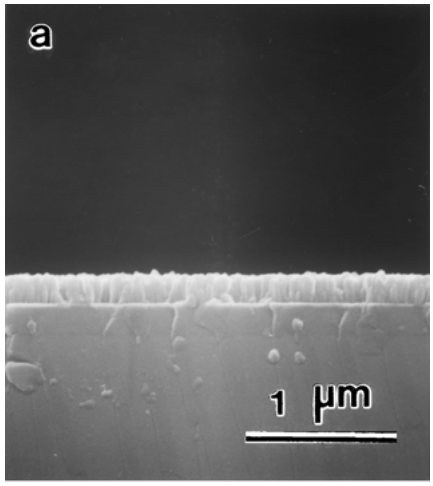

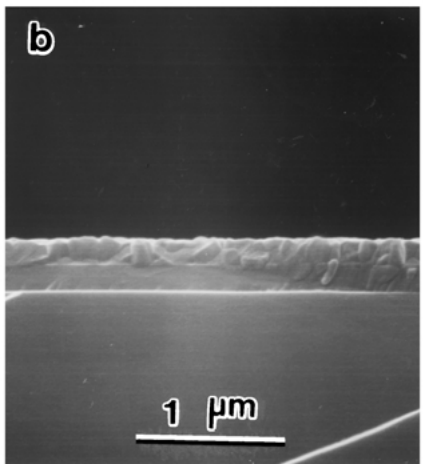

Figure 4 Cross-sectional micrograph of (a) RuO_2 thin film deposited at 315°C, note the columnar feature and (b) SrO thin film deposited at 550°C.

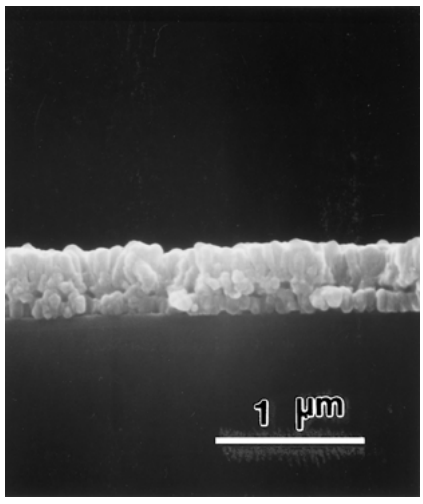

Figure 5 Cross-section of R295S550R295 film after annealing at 700°C 2 hrs. A thin SrO layer is sandwiched between two RuO_2 layer before annealing.

RuO_2 layers of equal thickness (0.22 μm) on the top and bottom of a thin SrO layer (0.1 μm thick). The sandwich was annealed at 700°C for 2 hrs. Its cross-section was shown in Fig. 5, which displays a thicker layer of larger grains on top of a thin layer of small grains. Evidently, the upper-layer thickness increases

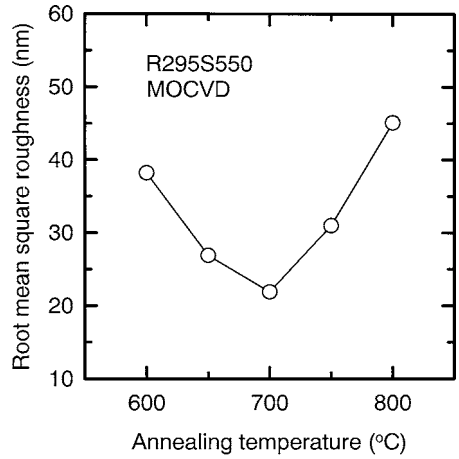

Figure 6 Root mean square roughness of the R295S550 surface versus annealing temperature.

and its grains grow larger with the help of ruthenium oxide vapor transported from the bottom layer.

3.2. Surface roughness and morphology

The surface roughness of R295S550 thin film, 280 nm thick, strongly depends on the annealing temperature. Fig. 6 indicates the root mean square roughness RMS of the $SrRuO_3$ film annealed at 700°C is the minimum, 22 nm. Above 700°C, the surface roughness increases with the annealing temperature owing to grain growth. The same trend was reported for the $SrRuO_3$ thin films prepared via pulsed laser deposition PLD. The RMS value of R295S550 after 800°C annealing is 45 nm, which is higher than that of PLD 800°C-deposited $SrRuO_3$ film 15 nm [20]. Below 700°C, the surface roughness increases with decreasing annealing temperature. The high surface roughness is attributed to large $SrCO_3$ grains, which form in the reaction between SrO and ambient CO_2. Fig. 7 illustrates the surface morphology of 600, 700, 800°C-annealed $SrRuO_3$ thin film, scanned by an atomic force microscope. The protruded, flaky grains on 600°C-annealed thin film are strontium carbonate crystals.

3.3. Film conductivity

The sheet resistivity of 700°C-annealed R295S550 with three cation ratios of Ru/(Ru + Sr), 0.5, 0.53, 0.55, is plotted in Fig. 8. The temperature dependence of Ru/(Ru + Sr) = 0.5 film resistivity exhibits the Curie point of $SrRuO_3$ crystal at ≈160 K [21, 22]. Its room-temperature sheet resisitivity is 910 $\mu\Omega$-cm, which is higher than the $SrRuO_3$ resistivity 280 $\mu\Omega$-cm reported by Okuda *et al.* [14]. The resistivity ratio, defined as ρ_{300K}/ρ_{17K}, is 1.92. When the cation ratio of Ru/(Ru + Sr) is increased to 0.53, no reflection of RuO_2 phase is detected under X-ray diffraction, the film resistivity is much reduced, the Curie transition also seems to be reduced to a lower temperature ≈90 K. The room-temperature resistivity is 470 $\mu\Omega$-cm. RuO_2 phase segregates if the Ru/(Ru + Sr) ratio is increased to 0.55, the sheet resistivity is further reduced, the Curie transitional kink vanishes. The room-temperature resistivity

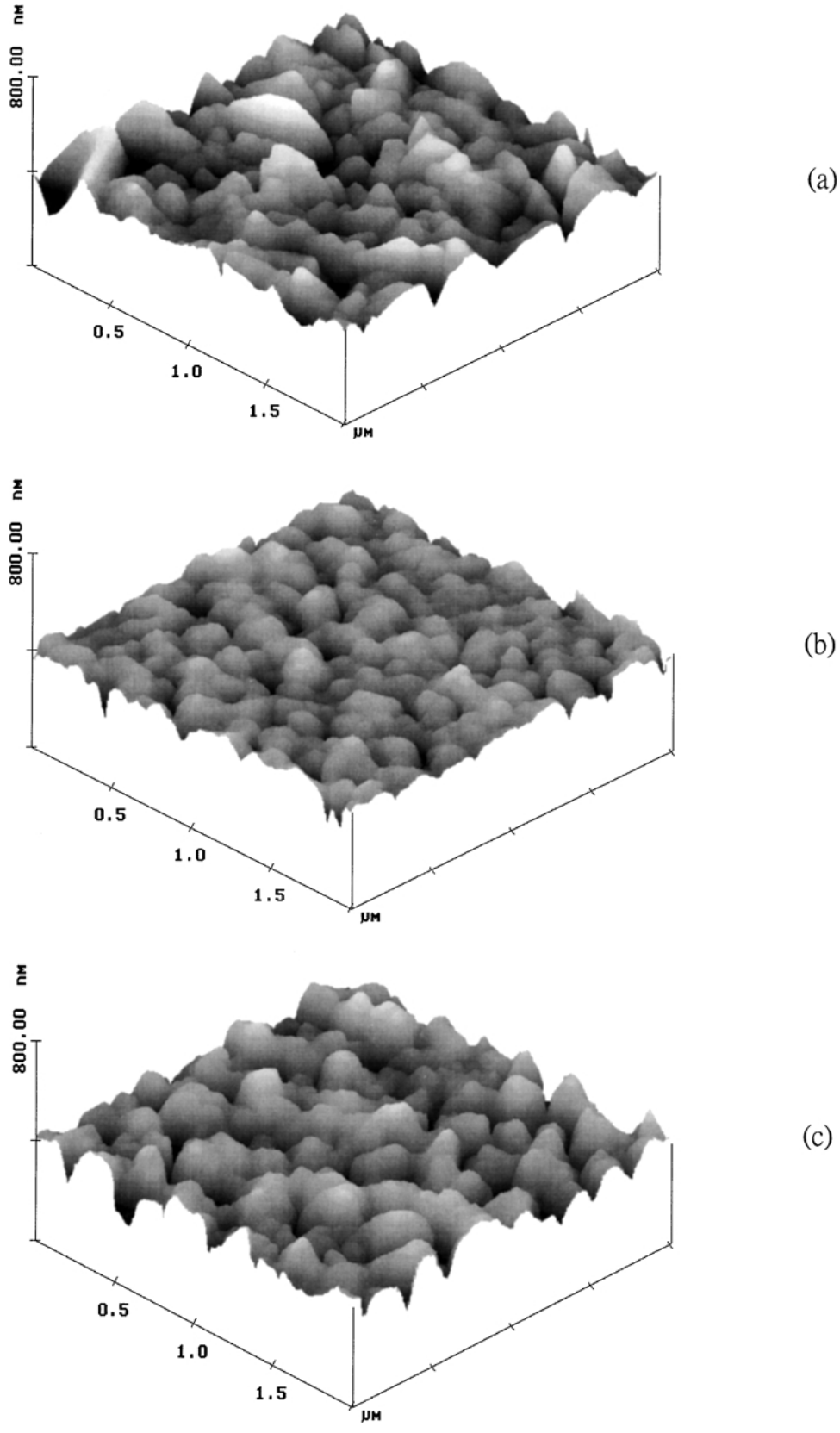

Figure 7 Surface morphology of the R295S550 surface annealed at (a) 600°C, (b) 700°C, and (c) 800°C. The $SrRuO_3$ thin film annealed at 700°C is optimum.

is 280 $\mu\Omega$-cm. The resistivity ratio ρ_{300K}/ρ_{17K} decreases to 1.4 for this Ru-rich composition.

4. Summary

Strontium ruthenate thin films are synthesized in a tubular hot-wall reactor, using consecutive deposition of ruthenium oxide and strontium oxide. The deposition sequence turns out to be a significant factor in the later high-temperature solid-state reaction. The columnar structure and the volatility of underlying ruthenium oxide facilitates the reaction between the component oxides, hence, the polycrystalline $SrRuO_3$ film is synthesized in 700°C annealing. The surface roughness

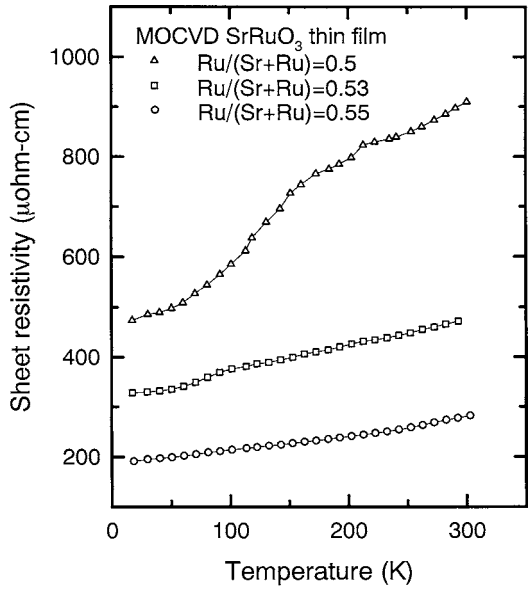

Figure 8 The film resistivities of 700°C-annealed R295S550 thin films.

of $SrRuO_3$ thin film is related to the annealing temperature. The 700°C-annealed $SrRuO_3$ film possesses a minimum surface roughness, RMS 22 nm. The resistivity ratio of stoichiometric $SrRuO_3$, defined as the resistivity at 300 K divided by the resistivity at 17 K, is around 1.92. The sheet resistivity and the resistivity ratio ρ_{300K}/ρ_{17K} both decrease as the Ru/(Sr + Ru) molar ratio increases.

Acknowledgements

The authors thank National Science Council of Taiwan and Chinese Petroleum Corporation for financial support through Project NSC89-CPC-7-011-012.

References

1. K. FUJIOKA, J. OKAMOTO, T. MIZOKAWA, A. FUJIMORI, I. HASE, M. ABBATE, H. J. LIN, C. T. CHEN, Y. TAKEDA and M. TAKANO, *Phys. Rev.* B **56** (1997) 6380.
2. P. B. ALLEN, H. BERGER, O. CHAUVET, L. FORRO, T. JARLBORG, A. JUNOD, B. REVAZ and G. SANTI, *ibid.* **53** (1996) 4393.
3. G. CAO, S. MCCALL, M. SHEPARD and J. E. CROW, *ibid.* **56** (1997) 321.
4. J. LIN, K. NATORI, Y. FUKUZUMI, M. IZUHA, K. TSUNODA, K. EGUCHI, K. HIEDA and D. MATSUNAGA, *Appl. Phys. Lett.* **76** (2000) 2430.
5. Z. R. DAI, S. Y. SON, B. S. KIM, D. K. CHOI and F. S. OHUCHI, *Mater. Res. Bull.* **34** (1999) 933.
6. M. IZUHA, K. ABE and N. FUKUSHIMA, *Jpn. J. Appl. Phys.* **36** (1997) 5866.
7. T. MORIMOTO, O. HIDAKA, K. YAMAKAWA, O. ARISUMI, H. KANAYA, T. IWAMOTO, Y. KUMURA, I. KUNISHIMA and S. TANAKA, *ibid.* **39** (2000) 2110.
8. M. KOBUNE, O. MATSUURA, T. MATSUZAKI and A. MINESHIGE, *ibid.* **39** (2000) 5451.
9. T. NISHIDA, S. OKAMURA, T. SHIOSAKI, S. FUJITA and Y. MASUDA, *ibid.* **38** (1999) 5337.
10. Q. X. JIA, F. CHU, C. D. ADAMS, X. D. WU, M. HAWLEY, J. H. CHO, A. T. FINDIKOGLU, S. R. FOLTYN, J. L. SMITH and T. E. MITCHELL, *J. Mater. Res.* **11** (1996) 2263.
11. C. B. EOM, R. J. CAVA, R. M. FLEMING, J. M. PHILLIPS, R. B. VAN DOVER, J. H. MARSHALL, J. W. P. HSU, J. J. KRAJEWSKI and W. F. PECK, *Science* **258** (1992) 1766.
12. R. BREITKOPF, L. J. MEDA, T. HAAS and R. U. KIRSS, in Proceedings of Materials Research Society (1998) Vol. 495, p. 51.
13. J. P. MERCURIO, J. H. YI, M. MANIER and P. THOMAS, *J. Alloys and Compounds* **308** (2000) 77.
14. N. OKUDA, K. SAITO and H. FUNAKUBO, *Jpn. J. Appl. Phys.* **39** (2000) 572.
15. W. C. SHIN and S. G. YOON, *J. Electrochem. Soc.* **144** (1997) 1055.
16. J. H. AHN, W. Y. CHOI, W. J. LEE and H. G. KIM, *Jpn. J. Appl. Phys.* **37** (1998) 284.
17. S. TRASATTI and W. E. O'GRADY, in "Advances in Electrochemistry and Electrochemical Engineering", edited by H. Gerischer and C. W. Tobias (Wiley-Interscience, New York, 1981) p. 184.
18. P. C. LIAO, S. Y. MAR, W. S. HO, Y. S. HUANG and K. K. TIONG, *Thin Solid Films* **287** (1996) 74.
19. R. S. CHEN, Y. S. HUANG, Y. L. CHEN and Y. CHI, *ibid.* **413** (2002) 85.
20. K. WATANABE, M. AMI and M. TANAKA, *Mater. Res. Bull.* **32** (1997) 83.
21. X. D. WU, S. R. FOLTYN, R. C. DYE, Y. COULTER and R. E. MUENCHAUSEN, *Appl. Phys. Lett.* **62** (1993) 2434.
22. R. J. BOUCHARD and J. L. GILLSON, *Mater. Res. Bull.* **7** (1972) 873.

Received 15 August 2002
and accepted 18 March 2003